JGR Atmospheres

RESEARCH ARTICLE
10.1029/2018JD028888

Key Points:
- Two approaches are developed to quantify the local contribution from primary emissions to haze using high-density site observations
- Both methods indicate the importance of local primary emissions in haze formation in an industrial city with contribution ratios of 0.4-0.7
- Local primary emission contribution ratio increases with mean pollution level during the winter of an industrial city

Correspondence to:
C. Zhao and Y. Wang,
czhao@bnu.edu.cn;
yuan.wang@caltech.edu

Citation:
Zhao, C., Wang, Y., Shi, X., Zhang, D., Wang, C., Jiang, J. H., Zhang, Q., & Fan, H. (2019). Estimating the contribution of local primary emissions to particulate pollution using high-density station observations. *Journal of Geophysical Research: Atmospheres*, *124*, 1648–1661. https://doi.org/10.1029/2018JD028888

Received 25 APR 2018
Accepted 10 JAN 2019
Accepted article online 15 JAN 2019
Published online 2 FEB 2019

Author Contributions:
Conceptualization: Chuanfeng Zhao
Data curation: Chunying Wang
Formal analysis: Chuanfeng Zhao, Xiaoqin Shi, Hao Fan
Funding acquisition: Chuanfeng Zhao
Investigation: Chuanfeng Zhao, Chunying Wang, Qiang Zhang
Methodology: Chuanfeng Zhao, Yuan Wang, Daizhou Zhang, Jonathan H. Jiang
Resources: Qiang Zhang
Supervision: Chuanfeng Zhao, Yuan Wang, Daizhou Zhang
Visualization: Chuanfeng Zhao
Writing - original draft: Chuanfeng Zhao
Writing – review & editing: Chuanfeng Zhao, Yuan Wang, Daizhou Zhang, Jonathan H. Jiang

Estimating the Contribution of Local Primary Emissions to Particulate Pollution Using High-Density Station Observations

Chuanfeng Zhao[1,2], Yuan Wang[2,3], Xiaoqin Shi[1], Daizhou Zhang[4], Chunying Wang[5], Jonathan H. Jiang[3], Qiang Zhang[6], and Hao Fan[1]

[1]State Key Laboratory of Earth Surface Processes and Resource Ecology and College of Global Change and Earth System Science, Beijing Normal University, Beijing, China, [2]Division of Geology and Planetary Science, California Institute of Technology, Pasadena, CA, USA, [3]Jet Propulsion Laboratory, California Institute of Technology, Pasadena, CA, USA, [4]Faculty of Environmental and Symbiotic Sciences, Prefectural University of Kumamoto, Kumamoto, Japan, [5]Hebei Sailhero Environmental Protection Hi-tech., Ltd, Shijiazhuang, China, [6]Department of Earth System Science, Tsinghua University, Beijing, China

Abstract Local primary emission, transport, and secondary formation of aerosols constitute the major atmospheric particulate matter (PM) over a certain region. To identify and quantify major sources of ambient PM is important for pollution mitigation strategies, especially on a city scale. We developed two source apportionment methods to make the first-order estimates of local primary contribution ratio (LCR) of $PM_{2.5}$ (PM with diameter less than 2.5 μm) using the high-density (about 1/km^2) network observations with high sampling frequency (about 1 hr). Measurements of $PM_{2.5}$ mass concentration from 169 sites within a 20 km × 20 km domain are analyzed. The two methods developed here are mainly based on the spatial and temporal variations of $PM_{2.5}$ within an urban area. The accuracy of our developed methods is subject to the assumptions on the spatial heterogeneity of primary and secondary formed aerosols as well as those from long-range transport to a city. We apply these two methods to a typical industrial city in China in winter of 2015 with frequent severe haze events. The local primary pollution contributions calculated from the two methods agree with each other that they are often larger than 0.4. The LCR range is from 0.4 to 0.7, with an average value of 0.63. Our study indicates the decisive role of locally emitted aerosols in the urban severe haze formation during the winter time. It further suggests that reductions of local primary aerosol emissions are essential to alleviate the severe haze pollution, especially in industrial cities.

1. Introduction

Haze pollution, caused primarily by fine suspended particulate matters (PM) in the air, has been a worldwide concern of the public, government, and scientists for many decades, with current hot spots in China and India (Y. Wang, Ma, et al., 2016; R. Zhang, Wang, et al., 2015). The PM, in particular those with aerodynamic size smaller than 2.5 μm ($PM_{2.5}$), can deteriorate atmospheric visibility, exert adverse effects on human health, and induce extreme weathers like drought and flooding (Cao, 2012; IPCC, 2013; Y. Wang, Zhang, & Saravanan, 2014, Y. Wang, Ma, et al., 2016; Xu et al., 2013; C. Zhao et al., 2018). To make reliable mitigation strategies for haze pollution, we need to improve our current understanding of the sources and formation of haze events and the contributions from different key factors.

Haze occurs as the accumulation of aerosol within the boundary layer under certain meteorological conditions, such as weak air movement and low boundary layer height (Sun et al., 2014; Y. S. Wang, Li, et al., 2014; X. J. Zhao et al., 2013; R. H. Zhang, Li, & Zhang, 2014; Q. Zhang, Quan, et al., 2015; Zheng et al., 2015). Aerosols can be classified into two groups according to the processes of their presence in the air: primary emitted and secondary formed. Primary ones are those directly emitted into the atmosphere from local sources and those transported from other places (e.g., X. Wang, Wen, et al., 2018, X. Wang, Liu, et al., 2018), and secondary ones are those produced in air via complicated chemistry and gas-to-particle conversions (Guo et al., 2014; Zhang et al., 2012; R. Zhang, Wang, et al., 2015) while the precursor gases could also be emitted locally or transported from other locations. Primary aerosols come from all kinds of natural and anthropogenic sources, such as wind-blown dust from desert, biomass burning, and fossil fuel combustion, among which the emission from industrial activities is considered as the significant source of $PM_{2.5}$ in

many regions (Al-Hasnawi et al., 2016; Ohara et al., 2007; Y. S. Wang, Li, Wang, et al., 2014). The formation of secondary aerosols is dependent on several factors, such as precursor gaseous species (SO_2, NO_x, NH_3, volatile organic compounds, etc.), sunlight, ambient relative humidity, temperature, and reaction surface (e.g., R. Zhang, Wang, et al., 2015). In addition to the aerosol sources, the abundance of $PM_{2.5}$ in a region also depends on their interplay with meteorology as indicated by almost all pollution studies (Yang et al., 2016).

A large number of studies have been carried out to untangle the dominant sources of pollutants in haze events of China, particularly for the Beijing-Tianjin-Hebei (BTH) region. Many of them reported the dominant role that secondary aerosol production plays in the elevation of $PM_{2.5}$ during severe haze episodes (e.g., Guo et al., 2014; Huang et al., 2014; Ma et al., 2017; Y. S. Wang, Li, et al., 2014; X. J. Zhao et al., 2013). For example, Huang et al. (2014) investigated the sources of $PM_{2.5}$ by using two receptor models, chemical mass balance (CMB) and positive matrix factorization (PMF), and showed high secondary aerosol contribution to haze events in China, particularly the BTH region. Guo et al. (2014) analyzed the chemical composition measurements by an aerosol mass spectrometer (AMS) with PMF method and found that gaseous emissions of volatile organic compounds and nitrogen oxides from traffic emissions and sulfur dioxide from regional industrial activities were responsible for secondary PM formation, while primary emissions and regional transport of PM were not very significant. Y. S. Wang, Li, et al. (2014) analyzed the $PM_{2.5}$ observations and the nonrefractory submicron aerosol species obtained from AMS during a heavy haze pollution episode over central and eastern China in January 2013 and suggested the main cause was the quick secondary transformation of primary gaseous pollutants to secondary aerosols, which contributed to the "explosive growth" and "sustained growth" of $PM_{2.5}$. Zheng et al. (2015) suggested that both secondary formation and regional transport play an important role in severe pollution events in addition to the synoptic weather patterns conductive to haze formation, by comprehensively analyzing the meteorology, aerosol chemical composition, and $PM_{2.5}$ mass concentration. With PMF analysis of measurements from an Aerosol Chemical Speciation Monitor, Sun et al. (2014) indicated that stagnant meteorological conditions, coal combustion, secondary production, and regional transport were four main factors driving the formation and evolution of haze pollution in Beijing during wintertime.

Models with the source apportionment capability can identify the haze contributions from local primary sources. For instance, it has been shown that Chemical Transport Model (CTM) can be accurately used to estimate single-source contributions (Li et al., 2018; H. Liu et al., 2017). In addition, there has been work to use a hybrid of dispersion modeling and CTM results to provide better fine-scale representation of pollutant concentrations. For example, recent model simulation studies (e.g., Appel et al., 2011; H. Zhang, Chen, et al., 2014) have investigated air quality based on high-resolution (4–12 km) simulations using the Community Multiscale Air Quality (CMAQ) model. The aerosol component of CMAQ model has been frequently used for the estimates of the primary emissions of elemental and organic carbon, dust, and other species (An et al., 2007; Binkowski & Roselle, 2003; Diaz-Robles et al., 2008; X. Li et al., 2015; Y. S. Wang, Li, Wang, et al., 2014; L. Wang et al., 2015; Woody et al., 2016). However, CTMs on the urban scale have their potential uncertainties. Several studies (e.g., Han et al., 2009; Kota et al., 2018; X. H. Liu et al., 2010; Tesche et al., 2006) have indicated that biases between CMAQ simulations and observations could exist due to potential uncertainties in emissions, simulated meteorology, chemical processes, etc.

Observational methods have also been developed to study air pollution or $PM_{2.5}$ contributions from different sources. Most of these methods make use of the aerosol chemical information with the PMF analysis (Aiken et al., 2008; Chen et al., 2014; Ge et al., 2012; He et al., 2010; Harrison et al., 2011; Y. X. Zhang et al., 2009). Q. Zhang, Quan, et al. (2015) showed that the conversion of SO_2 to sulfate accounts for 20% of $PM_{2.5}$ under humid conditions, implying likely more important contribution from primary emissions. Sun et al. (2014) found that secondary organic aerosols contributed 41–59% of organic aerosols with the rest being primary organic aerosols. Most of these quantification studies are source apportionment studies from aerosol chemical speciation measurements or estimated from model simulation studies. Issues exist for studies using Aerodyne AMS, which generally measures the relative chemical distributions for particles with diameters below 1.0 μm. As known, severe haze events are often accompanied with a large mass fraction from particles with diameters larger than 1.0 μm, but the source analysis from AMS provides figures of particles in submicron size only and cannot discriminate between source areas. Moreover, $PM_{2.5}$ source apportionment studies

can be carried out based on elemental analysis from filter sample measurements and back trajectory analysis from receptor model simulations. For example, Song et al. (2006) applied PMF to the source apportion of $PM_{2.5}$ and identified eight sources for $PM_{2.5}$ samples measured in Beijing area in 2000. Heo et al. (2009) carried out similar source apportionment analyses in Seoul, Korea, for 393 filter samples during the period from 2003 to 2006. Kalaiarasan et al. (2018) combined the elemental analysis based on filter samples and CMB model analysis to study the source apportionment of $PM_{2.5}$ in Manalore, India, and found that $PM_{2.5}$ in this region is mainly contributed by vehicle emissions. For studies with integrated filter-base samples, they focus on soluble materials, instead of nonsoluble metals, which could result in an impression of relatively higher contributions of secondary formation.

We here propose an observation-based approach, which is composed of a spatial approach and a temporal approach to estimate the relative contribution by local primary emissions to $PM_{2.5}$ for pollution events. Such an observation-based approach takes full advantage of the high-density network of $PM_{2.5}$ measurements recently deployed in several major cities in China.

2. Data and Methods

2.1. Data

Measurements of $PM_{2.5}$ mass concentration were performed at 169 sites, which are located within a 20-km × 20-km domain in an urban region of an industrial city in north China, from 2 November 2015 to 28 February 2016. The instruments have several modes to measure different variables, including $PM_{2.5}$, PM_{10}, SO_2, NO_2, CO, and O_3. In this study, the records of $PM_{2.5}$ were applied. The concentration of $PM_{2.5}$ was quantified with the β-ray absorption method. The measurable range is 5–2,000 $\mu g/m^3$, with resolution and accuracy of 0.01 and 1 $\mu g/m^3$, respectively. The temporal resolution for the observations was set at 1 hr. More information about the instrument are described by Shi et al. (2018). The spatial distribution of 169 sites is provided in Figure 1a. Figure 1b also shows the relative distribution of $PM_{2.5}$ emissions of four types of emission sources, including industry, power plant, residential, and transportation, from the multi-resolution emission inventory for China in 2015 (M. Li, et al., 2017). It is clear that industry emission is the largest source for this region.

We also classify the whole study period into 10 severe and 5 relatively weak haze periods based on the peak values of region-averaged hourly $PM_{2.5}$. Once the peak value of hourly $PM_{2.5}$ is larger than 350 $\mu g/m^3$, the whole haze event is classified as a severe haze period. The starting and ending of an event are defined as the $PM_{2.5}$ mass concentration overpasses and falls below 75 $\mu g/m^3$, respectively. Occasionally, there are cases with $PM_{2.5}$ mass concentration decreases first, and then increases with all $PM_{2.5}$ concentrations are higher than 75 $\mu g/m^3$, which are treated as one haze event here. If the peak value of $PM_{2.5}$ is less than 350 $\mu g/m^3$, the whole haze event from the starting to ending is classified as a relatively weak haze period. Table 1 shows the identified 10 severe and 5 relatively weak haze periods. For all haze events analyzed in this study, the haze event period is no less than 1 day and the daily mean $PM_{2.5}$ mass concentration on the day with peak hourly $PM_{2.5}$ should be higher than 75 $\mu g/m^3$. By contrast, a nonhaze event is defined as a period with $PM_{2.5}$ smaller than 75 $\mu g/m^3$ for at least 24 hr consecutively.

Meteorological factors such as wind and mixed-layer height can modulate the severity of pollution. For the domain and period of our interest in this study, we do not have concurrent weather station data and cannot get mixed-layer height and wind near surface. Instead, we obtain wind speed at 10 m above surface from the European Centre for Medium-Range Weather Forecasts (ECMWF) reanalysis data. Note that the grid box (40 km × 40 km) of ECMWF reanalysis data is even larger than our study domain (20 km × 20 km), so the wind from ECMWF only represents large-scale dynamics, not the urban scale. Figure 2 shows the relationship between study domain averaged $PM_{2.5}$ and grid wind speed at 10 m above surface from ECMWF. It shows that most wind speeds have values between 1 and 3 m/s, while wind directions are different. Thus, the wind speed near surface is generally less than 3 m/s during the haze events studied here. High wind speed sometimes occurs from northwest and northeast, generally with low $PM_{2.5}$ mass concentration. Figure 2 shows that there is no clear relationship between large-scale wind and $PM_{2.5}$ mass concentration for the study period. Due to the unavailability of surface observations, how meteorology affects the aerosol transport cannot be investigated in further detail.

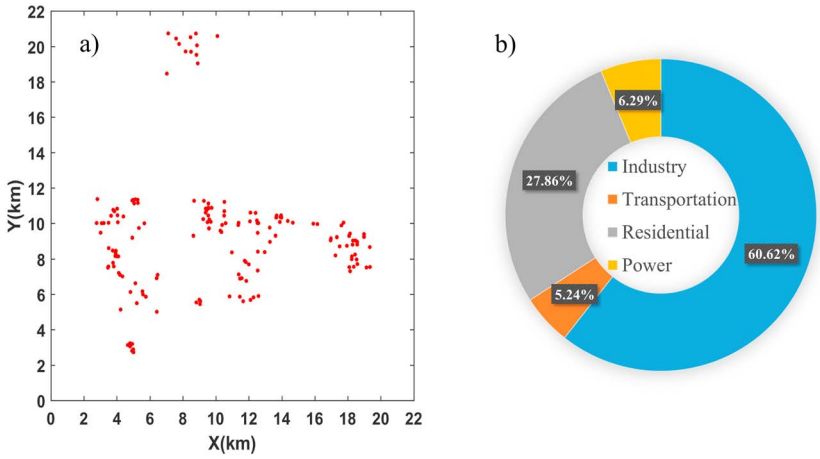

Figure 1. (a) The 169 ground observation stations with $PM_{2.5}$ measurements are shown with red points within a small domain of 20 km × 20 km; (b) the relative emissions of $PM_{2.5}$ from industry, transportation, residential, and power plants over the study domain.

2.2. Local Contribution Ratio Determination Methods

The sources of $PM_{2.5}$ can be divided into three types: local primary emissions, transport of aerosol particles, and local formed secondary particles. To quantify the local primary emission contribution fraction, we assume that the aerosol amount from transport (background amount) is uniform in space within a small domain area (DeGaetano & Doherty, 2004; Mohr et al., 2011; National Research Council, 2000), such as 20 km × 20 km in this study. For example, DeGaetano and Doherty (2004) showed little spatial variation in $PM_{2.5}$ mass concentrations in New York for regional-scale pollution processes. With a 20 km × 20 km study domain and a typical 3 m/s near surface wind speed, the dispersion time scale in this region is about 1.9 hr, which is much smaller than the duration time of a haze event studied here. Assuming the aerosols from transport vary little with location in the study domain could be valid. Regarding the secondary formation of aerosol, gas pollutants generally disperse through an urban area at the similar rates as particles. The formation of secondary PM species (e.g., secondary organic aerosol) can also depend on ambient $PM_{2.5}$ surface area and/or volume which impact heterogeneous chemistry and partitioning of semivolatile species (Kroll & Seinfeld, 2008; G. Wang, Zhang, et al., 2016). Hence, the mass concentration of the secondary formed $PM_{2.5}$ can be positively correlated with primarily emitted $PM_{2.5}$. With these in mind, we propose a spatial variation method and a temporal variation method to derive the local contribution ratio from primary emissions.

Table 1
The Severe (p) and Relatively Weak (c) Haze Time Periods Identified Subjectively Based on the $PM_{2.5}$ Concentrations, Along With the Time for Hourly $PM_{2.5}$ Peak Value, the Hourly $PM_{2.5}$ Peak Value, and the Time Duration (Days) for Each Haze Period

Serial number	Periods (yyyy.mm.dd)	$PM_{2.5}$ peaks of spatial mean value ($\mu g/m^3$)	Days
p1	2015.11.02–2015.11.07	403	6
p2	2015.11.07–2015.11.16	412	10
p3	2015.11.26–2015.12.03	839	8
p4	2015.12.03–2015.12.16	522	14
p5	2015.12.16–2015.12.27	808	12
p6	2015.12.27–2015.12.30	687	4
p7	2015.12.30–2016.01.05	732	7
p8	2016.01.08–2016.01.11	504	4
p9	2016.02.07–2016.02.15	381	9
p10	2016.02.18–2016.02.22	390	4
c1	2015.11.16–2015.11.26	284	11
c2	2016.1.5–2016.1.8	273	4
c3	2016.1.11–2016.2.7	344	28
c4	2016.2.15–2016.2.18	110	3
c5	2016.2.23–2016.2.28	310	6

We first quantify the local primary contribution fraction (LCR) based on the spatial heterogeneity of $PM_{2.5}$, which is defined as a spatial approach in this study. For any time during a haze event, we have one site with the minimum $PM_{2.5}$ mass concentration ($PM_{2.5min}$) over the analysis domain and a given site with $PM_{2.5}$ mass concentration ($PM_{2.5}$). Both $PM_{2.5}$ and $PM_{2.5min}$ are composed of three parts, local primary emission ($L\_PM_{2.5}$ and $L\_PM_{2.5min}$), transport of $PM_{2.5}$ ($T\_PM_{2.5}$ and $T\_PM_{2.5min}$), and secondary formation of $PM_{2.5}$ ($S\_PM_{2.5}$ and $S\_PM_{2.5min}$). The local primary emission contribution ratio can be defined as

$$LCRs_{i,t}^{def} = \frac{L\_PM_{2.5i,t}}{PM_{2.5i,t}} \qquad i = 1, 2, 3, ..., 169 \tag{1}$$

where i is the observation site and t is the observation time (hour). However, we do not have observation information of $L\_PM_{2.5}$. Instead, the local primary emission contribution ratio from analysis of spatial variation (LCRs) is calculated as

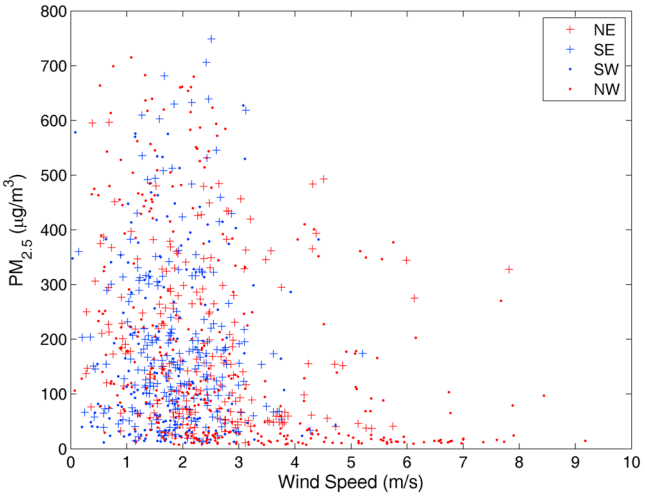

Figure 2. Scatter plot between near-surface grid wind speed at 10 m above the ground from the European Centre for Medium-Range Weather Forecasts and study domain averaged $PM_{2.5}$ mass concentration from November 2015 to February 2016. The red and blue "+" are for northeast (NE) and southeast (SE) winds, respectively; the red and blue "." are for northwest (NW) and southwest (SW) winds, respectively.

$$LCRs_{i,t} = \frac{PM_{2.5i,t} - PM_{2.5\,min t}}{PM_{2.5i,t}} \qquad i = 1, 2, 3, ..., 169 \tag{2}$$

The difference of $PM_{2.5}$ and $PM_{2.5min}$ can be written as $PM_{2.5} - PM_{2.5min} = L\_PM_{2.5} + T\_PM_{2.5} + S\_PM_{2.5} - L\_PM_{2.5min} - T\_PM_{2.5min} - S\_PM_{2.5min}$. With the assumption that aerosols from transport vary little with location in the study domain, $PM_{2.5} - PM_{2.5min} = L\_PM_{2.5} + S\_PM_{2.5} - L\_PM_{2.5min} - S\_PM_{2.5min}$. Thus, equation (2) can be written as

$$LCRs_{i,t} = \frac{L\_PM_{2.5i,t} - L\_PM_{2.5\,min t} + \left(S\_PM_{2.5i,t} - S\_PM_{2.5\,min t}\right)}{PM_{2.5i,t}} \qquad i = 1, 2, 3, ..., 169 \tag{3}$$

Compared to the definition of LCRs shown in equation (1), equation (2) includes two extra parts in the numerator, which are local primary emission at the site with minimum $PM_{2.5}$ and relative difference of secondary formation between the given site and the site with minimum $PM_{2.5}$. The local primary emission at the site with minimum $PM_{2.5}$ could make LCRs from equation (2) underestimated. In contrast, secondary formation terms between the given site and the site with minimum $PM_{2.5}$ could make LCRs overestimated since $S\_PM_{2.5}$ is generally larger than $S\_PM_{2.5min}$. Thus, the LCR probably includes some portion of the Secondary Organic Aerosol (SOA). However, the two terms work against with each other. We here assume their combination effect to LCRs is weak enough, so that they can be canceled out to a large extend. Thus, equation (2) can serve as a practical estimate of LCRs.

To evaluate the assumption of weak contribution from the two terms in equation (2), we conduct additional analyses on the available concurrent trace gas measurements. We calculate the ratios of variation (standard deviation) among 169 sites to their mean values for both NO_2 and $PM_{2.5}$, as shown in Figure 3a. The NO_2 demonstrates similar temporal variations as the $PM_{2.5}$. Another precursor gas of SO_2 exhibits very similar spatial variation as that of NO_2. Figure 3b further shows that the O_3 follows a similar temporal variation as the $PM_{2.5}$ with positive correlation. The results shown in Figure 3 imply that the secondary formed aerosols are positively correlated with $PM_{2.5}$ mass concentration. Moreover, Figure 3a shows that the ratios of

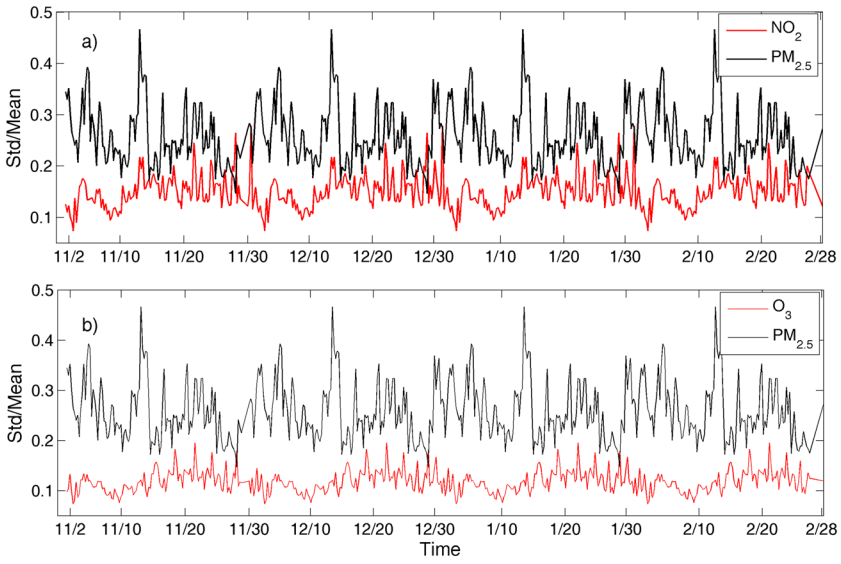

Figure 3. The temporal variation of the ratios of spatial variation (standard deviation) among 169 sites to their mean values for both NO_2 (red) and $PM_{2.5}$ (black) in panel (a) and for both O_3 (red) and $PM_{2.5}$ (black) in panel (b).

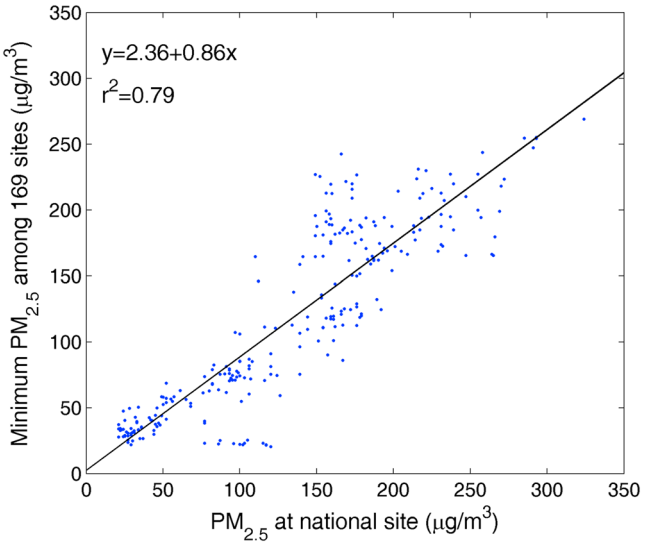

Figure 4. Comparison of the minimum $PM_{2.5}$ ($PM_{2.5min}$) mass concentration among the 169 sites within the study domain with the measured $PM_{2.5}$ mass concentration at a regional background site outside of the urban area.

variation (standard deviation) among 169 sites to their mean values are around 10–20% for most cases, much less than that for $PM_{2.5}$ which are around 20–40%. Figure 3b shows that the ratios of O_3 spatial variation (standard deviation) among 169 sites to their mean values are mainly 10–15%, even less than that for NO_2 and SO_2. These low values might further imply relatively weak spatial variation of secondary formed $PM_{2.5}$. In other words, the term S_$PM_{2.5}$-S_$PM_{2.5min}$ could have weak contribution in equation (2).

We further investigate the likely contribution from L_$PM_{2.5min}$ in equation (2). The site with $PM_{2.5min}$ is generally within a small domain with few emission sources, likely making $PM_{2.5min}$ close to the background values and L_$PM_{2.5min}$ close to 0. The accuracy of this argument could be examined by comparing the $PM_{2.5min}$ concentration to the one at a regional background site outside of the urban area. We here use the measurements from a national site outside of the urban area studied, while a few emission sources still exist at a few kilometers far away. As shown in Figure 4, the minimum $PM_{2.5}$ determined from the 169 sites in the study domain agrees very well ($r^2 = 0.79$) with that from the national site, with even a little smaller values. Thus, the $PM_{2.5min}$ should be with weak contribution from local primary emissions, even weaker than that for the national site. The relative larger values of $PM_{2.5}$ at the national site compared to $PM_{2.5min}$ should be associated with the existing emission sources around the national site, and using $PM_{2.5min}$ in our analysis could be more reasonable. Therefore, the magnitude of L_$PM_{2.5min}$ and (S_$PM_{2.5}$-S_$PM_{2.5min}$) are likely small, and they will be offset by each other in equation (2), making the LCRs reasonable to serve as a first-order estimate of local primary emission contribution ratio to the $PM_{2.5}$ during haze. Also note that invalid data, such as missing and bad data indicated in the data set, have been removed from our analysis.

We can also quantify the LCR based on the temporal evolution of the heterogeneity of $PM_{2.5}$ during a haze event. For any site in a given haze event, we can get the daily average $PM_{2.5}$ mass concentration at both peak ($PM_{2.5pk}$) and starting ($PM_{2.5st}$) stages. The growth amount of $PM_{2.5}$ at each site is $PM_{2.5pk}$-$PM_{2.5st}$, with the minimum growth amount $(PM_{2.5pk}\text{-}PM_{2.5st})_{min}$. With the similar assumptions and derivation processes as LCRs, the local primary emission contribution ratio from the temporal approach (LCRt) is calculated as

$$\mathrm{LCRt}_i = \frac{\left(\mathrm{PM}_{2.5pk_i} - \mathrm{PM}_{2.5st_i}\right) - \left(\mathrm{PM}_{2.5pk} - \mathrm{PM}_{2.5st}\right)_{\min}}{\mathrm{PM}_{2.5pk_i} - \mathrm{PM}_{2.5st_i}}, \quad i = 1, 2, 3, \ldots, 169 \tag{4}$$

where i is the observation site. Same as the LCRs from spatial approach, the LCRt from temporal approach is also a first-order estimate from observations.

2.3. Model Simulation Method

To compare with our observation-based estimates of local primary contributions we derived, we further carry out a dispersion model simulation combining the emission data set and the Weather Research and Forecast (WRF) with the Stochastic Time-Inverted Lagrangian Transport (STILT) model (WRF-STILT). The simulation domain is 900 km by 900 km with 3-km horizontal resolution. The main physical options in the WRF runs include the rapid radiative transfer scheme, the Yonsei University scheme for atmospheric boundary layer, and the Purdue Lin scheme for cloud microphysics, similar with our previous model setup (C. Zhao et al., 2009). The initial and boundary meteorology conditions for WRF are provided by the National Center for Environmental Prediction final analysis data. For STILT runs, we choose the receptor location at the center of the study region with the releasing height at 10 m. We first run the WRF to produce the hourly meteorology. Then, we run the STILT to get the 4-day-backward trajectories and footprints (f) every 3 hr. Third, we multiply the footprints with the a priori emission map (F) to get the $PM_{2.5}$ mass concentration from primary emissions within the city (local primary $PM_{2.5}$, $PM_{2.5lm}$) and outside the city (transport $PM_{2.5}$, $PM_{2.5tm}$) using the same method as indicated by C. Zhao et al. (2009),

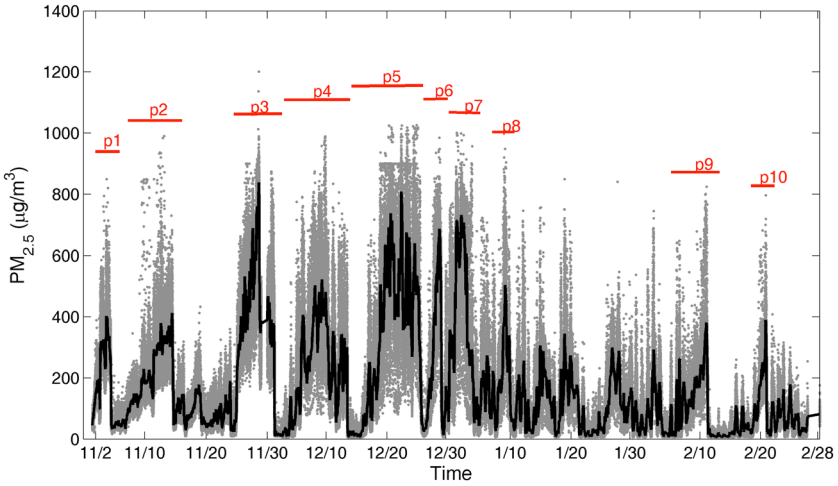

Figure 5. Time series of $PM_{2.5}$ observations from 169 sites (gray dots) along with the regional average of $PM_{2.5}$ (black line) during the winter period from 2 November 2015 to 28 February 2016. The marks with red lines indicated the severe haze events, and the time periods without marks are for relatively weak haze events.

$$C(X_r, t_r) = \sum_{i,j,m} f\left(X_r, t_r | x_i, y_j, t_m\right) \cdot F\left(x_i, y_j\right) \tag{5}$$

where X_r and t_r are receptor location and time, $f(X_r, t_r | x_i, y_j, t_m)$ is the footprint, and $F(x_i, y_j)$ is the surface emission map at location (x_i, y_j) and time t_m. Note that the a priori emission is from the multiresolution emission inventory for China in 2015. The $C(X_r, t_r)$ from the city contribution is $PM_{2.5lm}$, from the region outside the city is $PM_{2.5tm}$, and from all regions is total $PM_{2.5}$ from primary emissions and denoted as $PM_{2.5pm}$. Fourth, the model calculated relative contributions from local primary emission, transport of primary particles, and secondary formation can be obtained by

$$\begin{aligned} \mathrm{LCR}_m &= \frac{\mathrm{PM}_{2.5lm}}{\mathrm{PM}_{2.5}} \\ \mathrm{TCR}_m &= \frac{\mathrm{PM}_{2.5tm}}{\mathrm{PM}_{2.5}} \\ \mathrm{SCR}_m &= \frac{\mathrm{PM}_{2.5} - \mathrm{PM}_{2.5pm}}{\mathrm{PM}_{2.5}} \end{aligned} \tag{6}$$

where LCR_m, TCR_m, and SCR_m are model-based contributing ratios to total $PM_{2.5}$ from local primary emissions, transport of primary particles, and secondary formation, respectivley. $PM_{2.5}$ is the total observed $PM_{2.5}$ mass concentration.

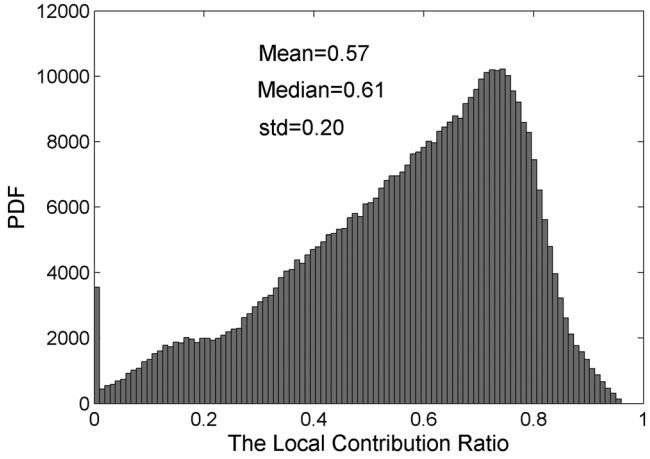

Figure 6. The probability distribution function (PDF) of local contribution ratio from primary emissions over all observation sites for all haze periods identified in Table 1 in winter 2015 using spatial approach. The mean, median, and standard deviation of the local contribution ratio from primary emissions are 0.57, 0.61, and 0.20, respectively.

3. Results and Discussion

Strong spatial and temporal variations of $PM_{2.5}$ have been found over a small domain. Figure 5 shows the temporal variation of $PM_{2.5}$ obtained from the 169 sites, along with the all-site averaged $PM_{2.5}$. The 10 sever haze events are marked in the figure, with remaining time periods for relatively weak haze events. It is clear that the $PM_{2.5}$ mass concentration was high in winter 2015 with identifying haze events which include starting, developing, peak, and dissipating stages. While all site observations show quite similar temporal variation, they did have large differences in the $PM_{2.5}$ mass concentrations, as demonstrated by gray points in Figure 5. The variability of $PM_{2.5}$ among the 169 sites are mostly 20–30% of their means. Large differences among the 169 sites are more distinct for those periods with high $PM_{2.5}$ mass concentration. These differences

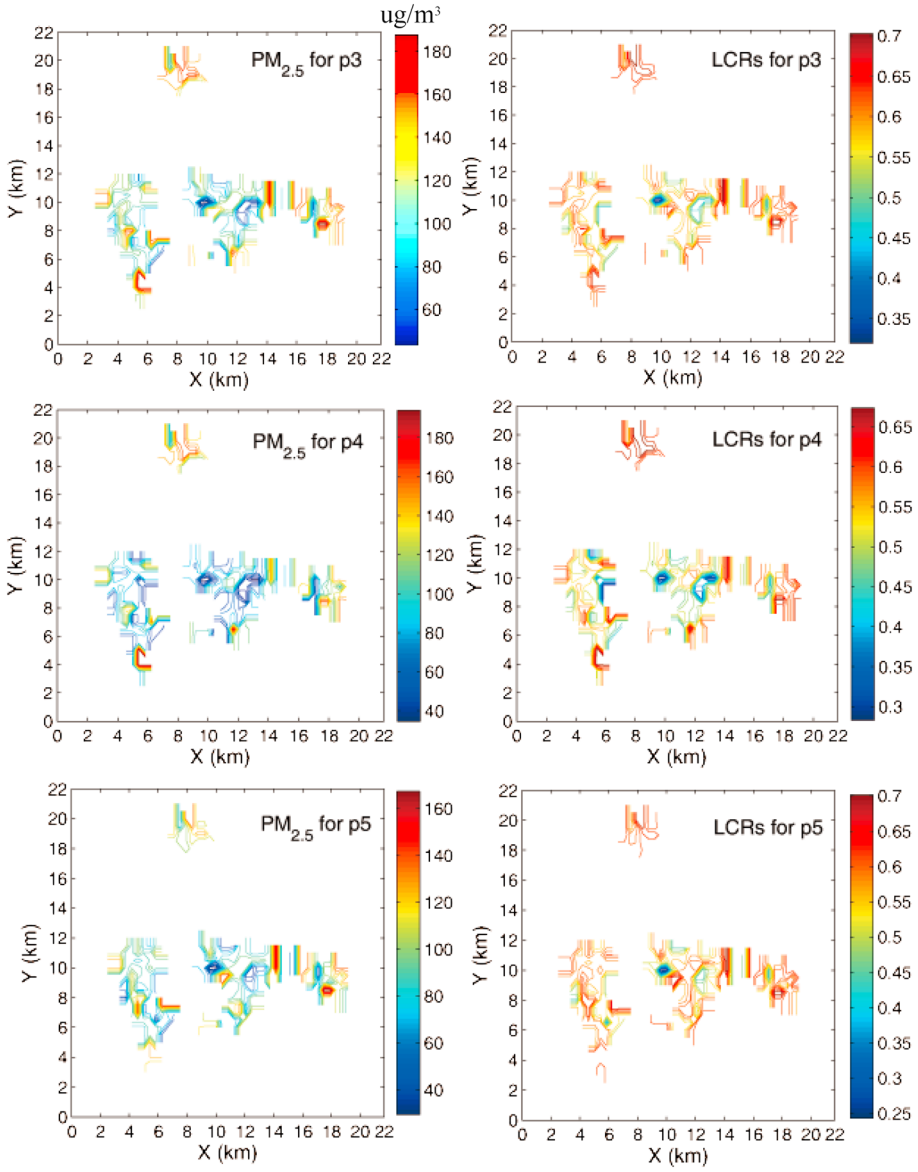

Figure 7. Spatial distribution of $PM_{2.5}$ (left column) and LCRs (right column) for three haze episodes of p3 (top row), p4 (middle row), and p5 (bottom row). LCR = local primary contribution ratio.

indicate the inhomogeneity of $PM_{2.5}$ mass concentration in a small domain, which should be associated with local primary emissions particularly when our assumptions in section 2 are reliable. The high mass concentration of $PM_{2.5}$ in winter in the BTH region was found by many previous studies (e.g., Sun et al., 2014; Y. S. Wang, Li, Wang, et al., 2014). Figure 5 also indicates that multiple haze events could exist during the time periods that are classified as relatively weak haze periods, which make the calculation of LCR from temporal approach challenging for these periods. Thus, the LCR from temporal approach is not examined for the relatively weak haze periods.

Large contribution ratio values from local primary emissions have been found for all study periods. Based on the spatial approach, the probability distribution function (PDF) of local contribution ratios from primary emissions over all observation sites during all haze events in winter 2015 shows a wide distribution with a mean (median) value of 0.57 (0.61) and standard deviation of 0.20, as shown in Figure 6. The maximum probability of LCRs is about 73%, which is also shown in Figure 6. The local primary aerosol emissions were the major contributor to the aerosol loadings within the examined region in winter 2015, with a contributing fraction of more than 60% in most periods.

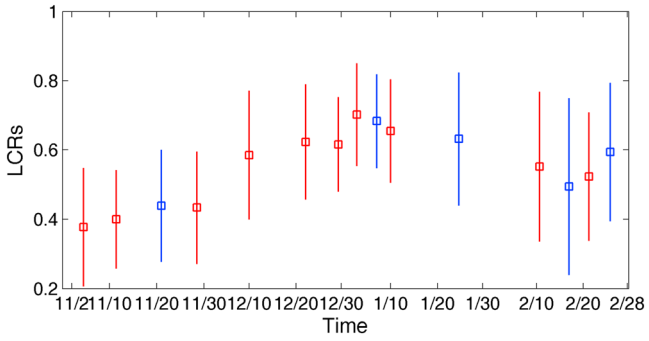

Figure 8. The temporal variation of the local contribution ratio from primary emissions using spatial approach (LCRs) in winter 2015. The squares represent the mean values among the observation sites with the study domain, and the bars represent the standard deviations. The red colors are for severe haze time with relatively high $PM_{2.5}$ concentrations, and the blue colors are for relatively weak haze time with relatively low $PM_{2.5}$ concentrations. The severe and relatively weak haze periods are defined in Table 1.

We investigated the spatial distribution of LCRs for all severe and relatively weak haze periods. Figure 7 shows the distributions for three of severe haze events: p3, p4, and p5. From this figure, we can see more clearly that LCRs are correlated with the $PM_{2.5}$ mass concentrations: They demonstrated very similar patterns while slight differences exist. Moreover, the spatial patterns of LCRs are generally similar among haze episodes. Actually, the LCRs for other episodes also demonstrate similar spatial patterns, while some differences do exist. These similar spatial patterns of $PM_{2.5}$ and LCRs indicate the relatively stable pollution sources in this study domain. The exact pollution sources types in different locations are not investigated in this study since we do not have the pollution source information.

Figure 8 shows the temporal variation of averaged LCRs using the spatial approach, which includes both the severe and weak haze events. While there are a relatively large range of values, the LCRs show a clear temporal/monthly variation with the maximum local primary contribution ratio about 70% in late December and early January. LCRs shows the minimum value about 40% in early November before the season with coal burning for heating which starts on November 15. This result implies that local primary contribution ratio could increase with the pollution level. However, if we compare the LCRs between severe and weak haze events at periods close to each other, no significant differences were found. This implies that the local primary emission contributions are similar within a short time window while the haze strength could be different due to various meteorology. We should note that local meteorology could affect the transport and secondary formation of aerosols and make LCR vary with meteorology, which is not discussed in this study. In fact, heavy haze events often occur under stable weather conditions, that is, stagnant airflow, under which there are much less regional aerosol transports and dispersions. Figure 9 shows the scatter plot between mean $PM_{2.5}$ mass concentration and LCRs for all identified haze periods in winter of December, January, and February. We can find a good linear relationship between LCRs and $PM_{2.5}$ mass concentration ($y = 0.54 + 0.0004x$) with correlation coefficient 0.61. The intercept is larger than 0.5, and the slope is positive, suggesting that local primary emission contribution ratio of aerosols increases with pollution level and local primary emission is generally the largest $PM_{2.5}$ influential factor with contributions larger than 54% for the study period. The correlation coefficient of 0.61 corresponds to an r^2 value of 0.37, which means that 37% of the variability of domain averaged $PM_{2.5}$ can be attributed to changes in the mean LCRs for the study region. Other influential factors to LCRs will be investigated in future, particularly the meteorology.

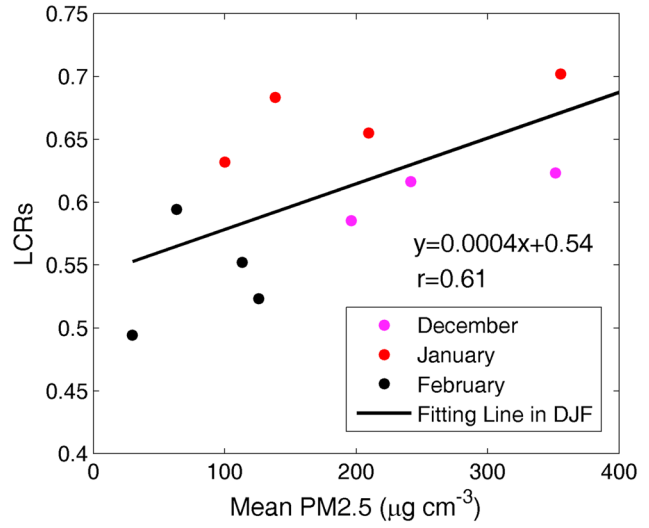

Figure 9. Variation of local contribution ratio (LCRs) from primary emissions with the pollution levels in winter time of December, January, and February (DJF), along with the linear fitting regression line. Both severe and relatively weak haze events have been adopted in this analysis.

Figure 10 shows more details about the PDF of LCRs at all observation sites during different pollution periods as defined in Table 1 using the spatial approach. The mean and median values of LCRs for each period have also been listed in the panels. Same as those indicated earlier, only for the four haze events (p1, p2, p3, and c1) in November, the LCRs values with maximum PDF are less than 0.5. For other haze events (p4–p10, c2–c5) in December, January, and February, the LCRs values with maximum PDF are almost all larger than 0.5, indicating significant $PM_{2.5}$ contribution from local primary emissions. Also, note that the LCRs demonstrate various shapes for their PDFs. Among the 15 haze cases, while most demonstrate single-mode distribution, weak bimodality distributions could be found for a few haze events. This could be associated with the hot spots of local strong emission sources in an industrial city. For those haze events with relatively larger heterogeneity, the sites near the strong emission spots and relatively far away from those spots shows large differences in the local primary emission contribution values, large versus small, causing two peak values in the PDF distribution of LCRs.

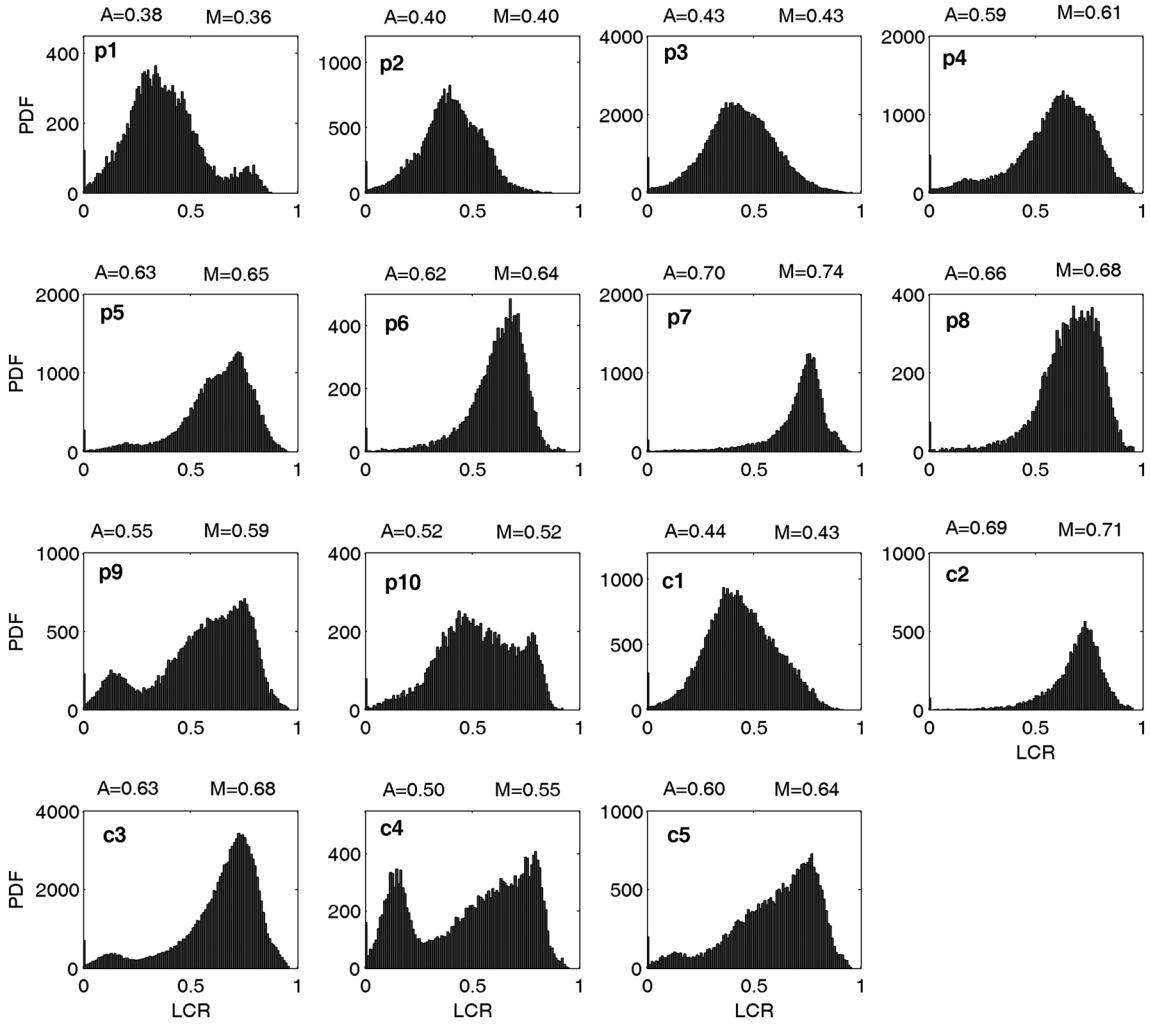

Figure 10. The probability density function (PDF) of local contribution ratio (LCRs) from primary emissions over all observation sites for 10 severe haze events marked with "p" and 5 relatively weak haze events marked with "c," same as defined in Table 1 using spatial approach. The mean (*A*) and median (*M*) values of LCRs for each period have also been listed above the panels.

The temporal variation of LCRt for identified severe haze periods is analyzed in Figure 11. There is also a clear temporal variation of LCRt, with the maximum value around 70% in late December and early January and the minimum value around 40% in early November and late February. The LCRt values and their temporal variation are similar to those obtained from spatial approach. In addition to the temporal variation of LCRt, the spatial variation of LCRt is also examined for each episode. They are roughly consistent with that for LCRs. By checking the LCRs and LCRt values for 10 haze events, we found that LCRs and LCRt consistently show that local primary contributions are larger than 40% for most sites. The approaches could be potentially improved for a more accurate estimation in the future, including reducing assumptions by adding information of the spatial distribution of aerosols from transport and secondary formation.

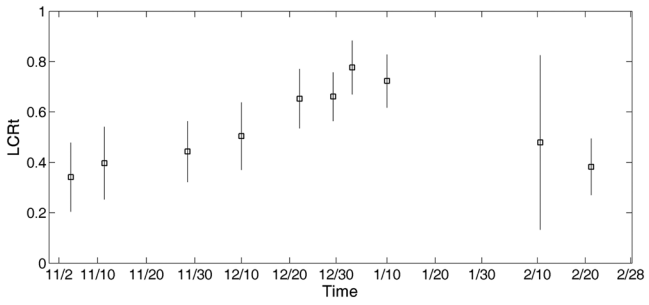

Figure 11. The temporal variation of the local contribution ratio from primary emissions using temporal approach (LCRt) for identified severe haze periods in winter 2015. The squares represent the mean values among the observation sites with the study domain, and the bars represent the standard deviations.

Figure 12 shows the 4-month averaged maps of WRF-STILT footprints from 2 November 2015 to 28 February 2016. It clearly shows that the most influential region to the receptor location (or study domain) is the study city. For regions outside the city, the footprints are much smaller. It

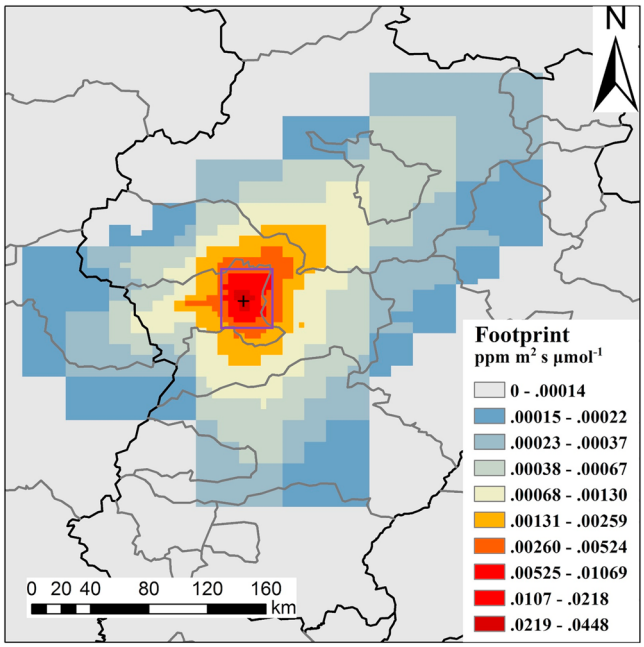

Figure 12. The 4-day-backward footprint maps averaged over 4 months near the study city (purple squares) with the high-density particulate matter observation network. "+" denotes the receptor location.

implies that for primary aerosol particles, local emissions could play a much more important role than transport from outside regions. Figure 13 further shows the PDFs of LCR_m, TCR_m, and SCR_m, along with the average relative contributions from local primary emission, transport of primary particles, and secondary formation for the whole study period. The local primary contribution ratio from the model simulation is mainly between 20% and 80%, with an average value of 51.4% and a standard deviation of 19%. Note that our observation-based analyses have shown a wide distribution of LCR with a mean value of 0.57 with standard deviation of 0.20, roughly consistent with the model-based estimates. A two-tailed Student's t test shows that the observation-based LCRs are (not) statistically different from the model-based estimates at the 95% (99%) significance level. Although uncertainties could exist for both the observation-based estimates and model simulation results, their consistency in LCR contributions help justify the new methodology introduced in this study. On average, the relative contributions from local primary emission, transport of primary particles, and secondary formation are 51.4%, 16.8%, and 31.8% with standard deviations of 19%, 10%, and 20%, respectively (Figure 13).

We also compared our results with previous studies while there are slight differences in the study locations. Liu et al. (2016) showed that the primary emission contributions to the $PM_{2.5}$ in the BTH region where our study domain lies within is about 68 ± 12% in the winter of 2010 based on the Weather Research and Forecasting model with Chemistry simula-

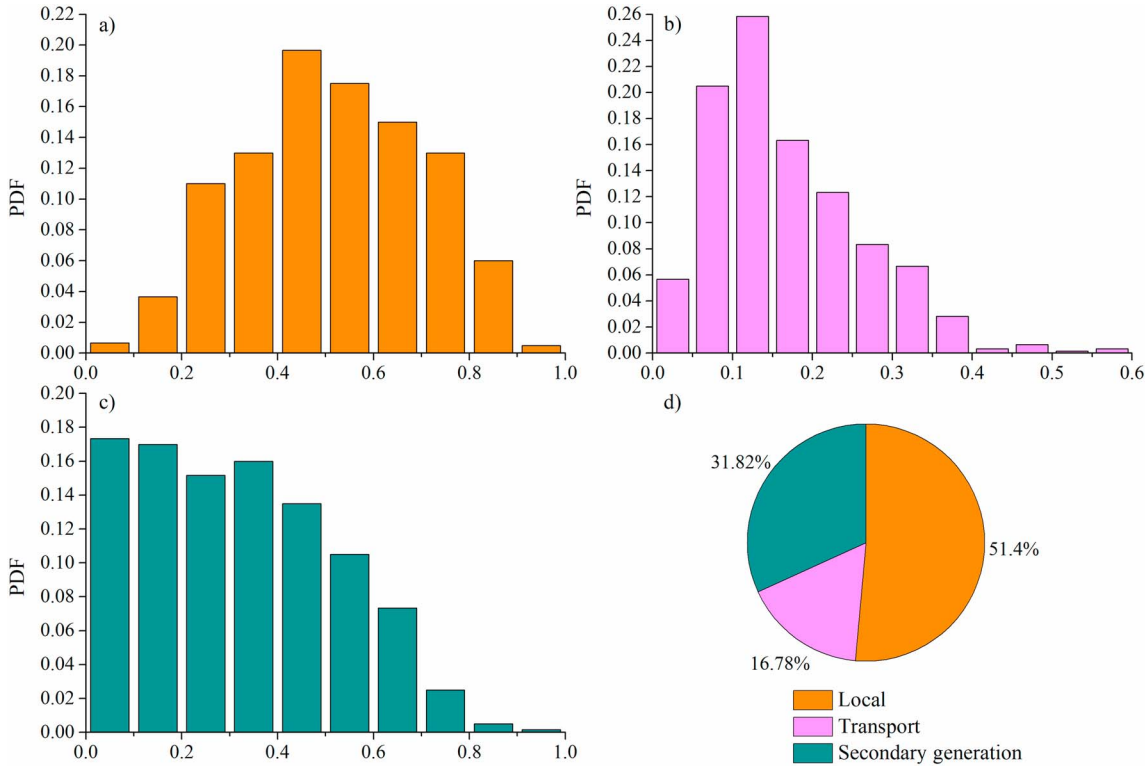

Figure 13. Normalized PDFs of model-based contributing ratios to total $PM_{2.5}$ from (a) local primary emissions, (b) transport of primary particles, and (c) secondary formation, along with (d) the averaged relative contributions from these three sources for the 4-month period from 2 November 2015 to 28 February 2016. PDF = probability density function.

tion study. This result is roughly consistent with the average values of our findings (Figure 9) though it is slightly larger. Note that emission controls may have decreased the local emission amount in 2015 compared to that in 2010, and the primary emissions in the study of Liu et al. (2016) include both local and transported. Differently, some studies (e.g., Guo et al., 2014) showed slightly more significant contributions (33–54%) from secondary formation in Beijing compared to our model-based estimates for the examined industrial city. Note that Beijing is a city with much less industries compared to the one we studied. Currently, it is still challenging for us to accurately evaluate the results due to the lack of direct measurements and source apportionment of aerosols from local primary emissions, the secondary formation, and the regional transport.

4. Conclusions

This study develops two $PM_{2.5}$ spatiotemporal variation analysis methods to provide a first-order estimate of the local primary emission contribution ratio to $PM_{2.5}$ using high-density network observations with high sampling frequency. These methods are applied to $PM_{2.5}$ observations in an industrial city of north China. Both methods show that the contribution of locally emitted aerosols is significantly high in all haze events from November 2015 to February 2016, with a mean ratio larger than 60%. The analyses from the two methods show similar LCR values and seasonal variations, with maximum values around 0.70 in late December and early January and minimum values around 0.40 in early November. It is also found that the local contribution ratio of primary emissions increases with pollution level, with a positive correlation coefficient of 0.61 in the winter time. Further model-based simulation analyses show roughly consistent results as the observation-based estimates regarding the local primary emission contributions to $PM_{2.5}$. Our results suggest that local primary emissions play a critical role in the high $PM_{2.5}$, particularly during severe haze events in an industrial type of city. One implication of our study is that control of local primary emission should be an important strategy to alleviate the China haze pollution, particularly for the industrial urban regions. Our methods of quantifying the $PM_{2.5}$ source apportionment of local primary emissions using high-density station observations provides an effective means for air quality assessment and decision-making support.

Acknowledgments
This work was supported by the National Key R&D Program on Monitoring, Early Warning and Prevention of Major Natural Disasters under grant 2017YFC1501403, the National Natural Science Foundation of China under grant 41575143, the State Key Laboratory of Earth Surface Processes and Resource Ecology (2017-ZY-02), and the Fundamental Research Funds for the Central Universities (2017EYT18 and 312231103). The authors also acknowledge the support by the Division of Geology and Planetary Science, California Institute of Technology (Caltech), as well as the support by the Caltech Jet Propulsion Laboratory, sponsored by NASA. The data used in this study are available by request to Chuanfeng Zhao through czhao@bnu.edu.cn or directly downloaded from ftp: nwpc.nmc.cn under directory zhao_paper_data. We acknowledge the helpful discussions with David Diner at Jet Propulsion Laboratory and Yuanlong Huang and Lu Xu at Caltech. We also thank the three anonymous reviewers for their constructive comments.

References

Aiken, A. C., DeCarlo, P. F., Kroll, J. H., Worshnop, D. R., Huffman, J. A., Docherty, K. S., et al. (2008). O/C and OM/OC ratios of primary, secondary, and ambient organic aerosols with high-resolution time-of-flight aerosol mass spectrometry. *Environmental Science & Technology*, *42*(12), 4478–4485. https://doi.org/10.1021/es703009q

Al-Hasnawi, S. S., Hussain, H. M., Al-Ansari, N., & Knutsson, S. (2016). The effect of the industrial activities on air pollution at Baiji and its surrounding areas, Iraq. *Engineering*, *8*, 34–44. https://doi.org/10.4236/eng.2016.81004

An, X., Zhu, T., Wang, Z., Li, C., & Wang, Y. (2007). A modeling analysis of a heavy air pollution episode occurred in Beijing. *Atmospheric Chemistry and Physics*, *7*(12), 3103–3114. https://doi.org/10.5194/acp-7-3103-2007

Appel, K. W., Foley, K. W., Bash, J. O., Pinder, R. W., Dennis, R. L., Allen, D. J., & Pickering, K. (2011). A multi-resolution assessment of the Community Multiscale Air Quality (CMAQ) model v4.7 wet deposition estimates for 2002–2006. *Geoscientific Model Development*, *4*(2), 357–371. https://doi.org/10.5194/gmd-4-357-2011

Binkowski, F. S., & Roselle, S. J. (2003). Models-3 Community Multiscale Air Quality (CMAQ) model aerosol component 1. Model description. *Journal of Geophysical Research*, *108*(D6), 4183. https://doi.org/10.1029/2001JD001409

Cao, J. J. (2012). Pollution status and control strategies of $PM_{2.5}$ in China. *Journal of Earth and Environment*, *3*, 1030–1036.

Chen, W. T., Shao, M., Lu, S. H., Wang, M., Zeng, L. M., Yuan, B., & Liu, Y. (2014). Understanding primary and secondary sources of ambient carbonyl compounds in Beijing using the PMF model. *Atmospheric Chemistry and Physics*, *14*(6), 3047–3062, https://doi.org/10.5194/acp-14-3047-2014

DeGaetano, A. T., & Doherty, O. M. (2004). Temporal, spatial and meteorological variations in hourly $PM_{2.5}$ concentration extremes in New York City. *Atmospheric Environment*, *38*(11), 1547–1558. https://doi.org/10.1016/j.atmosenv.2003.12.020

Diaz-Robles, L. A., Fu, J. S., & Reed, G. D. (2008). Modeling and source apportionment of diesel particulate matter. *Environmental International*, *34*(1), 1–11. https://doi.org/10.1016/j.envint.2007.06.002

Ge, X., Setyan, A., Sun, Y., & Zhang, Q. (2012). Primary and secondary organic aerosols in Fresno, California during wintertime: Results from high resolution aerosol mass spectrometry. *Journal of Geophysical Research*, *117*, D19301. https://doi.org/10.1029/2012JD018026

Guo, S., Hu, M., Zamora, M. L., Peng, J., Shang, D., Zheng, J., Du, Z., et al. (2014). Elucidating severe urban haze formation in China. *Proceedings of the National Academy of Sciences of the United States of America*, *111*(49), 17373–17378. https://doi.org/10.1073/pnas.1419604111

Han, K. M., Song, C. H., Ahn, H. J., Park, R. S., Woo, J. H., Lee, C. K., et al. (2009). Investigation of NO_x emissions and NO_x-related chemistry in East Asia using CMAQ-predicted and GOME-derived NO_2 columns. *Atmospheric Chemistry and Physics*, *9*(3), 1017–1036. https://doi.org/10.5194/acp-9-1017-2009

Harrison, R. M., Beddows, D. C. S., & Dall'Osto, M. (2011). PMF analysis of wide-range particle size spectra collected on a major highway. *Environmental Science & Technology*, *45*(13), 5522–5528. https://doi.org/10.1021/es2006622

He, L. Y., Lin, Y., Huang, X. F., Guo, S., Xue, L., Su, Q., et al. (2010). Characterization of high-resolution aerosol mass spectra of primary organic aerosol emissions from Chinese cooking and biomass burning. *Atmospheric Chemistry and Physics*, *10*(23), 11535–11543, https://doi.org/10.5194/acp-10-11535-2010

Heo, J.-B., Hopke, P. K., & Yi, S.-M. (2009). Source apportionment of PM2.5 in Seoul, Korea. *Atmospheric Chemistry and Physics*, *9*, 4957–4971. https://doi.org/10.5194/acp-9-4957-2009

Huang, R. J., Zhang, Y., Bozzetti, C., Ho, K. F., Cao, J. J., Han, Y., et al. (2014). High secondary aerosol contribution to particulate pollution during haze events in China. *Nature*, *514*(7521), 218–222. https://doi.org/10.1038/nature13774

Intergovernmental Panel on Climate Change (IPCC) (2013). *Climate change 2013: The physical science basis. Contribution of Working Group I to the Fifth Assessment Report of the Intergovernmental Panel on Climate Change*. Cambridge, U.K. and New York, U.S.A: Cambridge University Press. http://www.ipcc.ch/report/ar5/wg1/ (accessed Jan 2, 2015)

Kalaiarasan, G., Balakrishnan, R. M., Sethunath, N. A., & Manoharan, S. (2018). Source apportionment studies on particulate matter (PM10 and PM2.5) in ambient air of urban Mangalore, India. *Journal of Environmental Management*, *217*, 815–824. https://doi.org/10.1016/j.jenvman.2018.04.040

Kota, S., Guo, H., Myllyvirta, L., Hu, J., Sahu, S., Garaga, R., et al. (2018). Year-long simulation of gaseous and particulate air pollutants in India. *Atmospheric Environment*, *180*, 244–255. https://doi.org/10.1016/j.atmosenv.2018.03.003

Kroll, J. H., & Seinfeld, J. H. (2008). Chemistry of secondary organic aerosol: Formation and evolution of low-volatility organics in the atmosphere. *Atmospheric Environment*, *42*(16), 3593–3624. https://doi.org/10.1016/j.atmosenv.2008.01.003

Li, M., Zhang, Q., Kurokawa, J.-I., Woo, J.-H., He, K., Lu, Z., et al. (2017). MIX: A mosaic Asian anthropogenic emission inventory under the international collaboration framework of the MICS-Asia and HTAP. *Atmospheric Chemistry and Physics*, *17*(2), 935–963. https://doi.org/10.5194/acp-17-935-2017

Li, X., Wu, J., Elser, M., Feng, T., Cao, J., El-Haddad, I., et al. (2018). Contributions of residential coal combustion to the air quality in Beijing-Tianjin-Hebei (BTH), China: a case study. *Atmospheric Chemistry and Physics*, *18*, 10,675–10,691. https://doi.org/10.5194/acp-18-10675-2018

Li, X., Zhang, Q., Zhang, Y., Zheng, B., Wang, K., Chen, Y., et al. (2015). Source contributions of urban $PM_{2.5}$ in the Beijing–Tianjin–Hebei region: Changes between 2006 and 2013 and relative impacts of emissions and meteorology. *Atmospheric Environment*, *123*, 229–239. https://doi.org/10.1016/j.atmosenv.2015.10.048

Liu, H., He, J., Guo, J., Miao, Y., Yin, J., Wang, Y., et al. (2017). The blue skies in Beijing during APEC 2014: A quantitative assessment of emission control efficiency and meteorological influence. *Atmospheric Environment*, *167*, 235–244. https://doi.org/10.1016/j.atmosenv.2017.08.032

Liu, J., Mauzerall, D. L., Chen, Q., Zhang, Q., Song, Y., Peng, W., et al. (2016). Air pollutant emissions from Chinese households: A major and underappreciated ambient pollution source. *Proceedings of the National Academy of Sciences of the United States of America*, *113*(28), 7756–7761. https://doi.org/10.1073/pnas.1604537113

Liu, X. H., Zhang, Y., Cheng, S. H., Xing, J., Zhang, Q., Streets, D. G., et al. (2010). Understanding of regional air pollution over China using CMAQ, part I performance evaluation and seasonal variation. *Atmospheric Environment*, *44*(20), 2415–2426. https://doi.org/10.1016/j.atmosenv.2010.03.035

Ma, Q., Wu, Y., Zhang, D., Wang, X., & Zhang, R. (2017). Roles of regional transport and heterogeneous reactions in $PM_{2.5}$ increase during haze episodes in Beijing. *The Science of Total Environment*, *599-600*, 246–253. https://doi.org/10.1016/j.scitotenv.2017.04.193

Mohr, C., Richter, R., DeCarlo, P. F., Prevot, A. S. H., & Baltensperger, U. (2011). Spatial variation of chemical composition and sources of submicron aerosol in Zurich during wintertime using mobile aerosol mass spectrometer data. *Atmospheric Chemistry and Physics*, *11*(15), 7465–7482. https://doi.org/10.5194/acp-11-7465-2011

National Research Council (2000). *Waste incineration and public health*. Washington DC: National Academy Press.

Ohara, T., Akimoto, H., Kurokawa, J., Horii, N., Yamaji, K., Yan, X., & Hayasaka, T. (2007). An Asian emission inventory of anthropogenic emission sources for the period 1980–2020. *Atmospheric Chemistry and Physics*, *7*, 4419–4444. https://doi.org/10.5194/acp-7-4419-2007

Shi, X., Zhao, C., Wang, C., Jiang, J. H., & Yung, Y. L. (2018). A method of examination about the spatial representation of $PM_{2.5}$ obtained from a network of limited surface stations. *Journal of Geophysical Research: Atmospheres*, *123*, 3145–3158. https://doi.org/10.1002/2017JD027913

Song, Y., Zhang, Y., Xie, S., Zeng, L., Zheng, M., Salmon, L. G., et al. (2006). Source Apportionment of PM2.5 in Beijing by Positive Matrix Factorization. *Atmospheric Environment*, *40*, 1526–1537. https://doi.org/10.1016/j.atmosenv.2005.10.039

Sun, Y., Jiang, Q., Wang, Z., Fu, P., Li, J., Yang, T., & Yin, Y. (2014). Investigation of the sources and evolution processes of severe haze pollution in Beijing in January 2013. *Journal of Geophysical Research: Atmospheres*, *119*, 4380–4398. https://doi.org/10.1002/2014JD021641

Tesche, T. W., Morris, R., Tonnesen, G., McNally, D., Boylan, J., & Brewer, P. (2006). CMAQ/CAMx annual 2002 performance evaluation over the eastern US. *Atmospheric Environment*, *40*(26), 4906–4919. https://doi.org/10.1016/j.atmosenv.2005.08.046

Wang, G., Zhang, R., Gomez, M. E., Yang, L., Levy Zamora, M., Hu, M., Lin, Y., et al. (2016). Persistent sulfate formation from London fog to Chinese haze. *Proceedings of the National Academy of Sciences of the United States of America*, *113*(48), 13630–13635. https://doi.org/10.1073/pnas.1616540113

Wang, L., Wei, Z., Wei, W., Fu, J. S., Meng, C., & Ma, S. (2015). Source apportionment of $PM_{2.5}$ in top polluted cities in Hebei, China using the CMAQ model. *Atmospheric Environment*, *122*, 723–736. https://doi.org/10.1016/j.atmosenv.2015.10.041

Wang, X., Liu, J., Che, H. Z., Ji, F., & Liu, J. J. (2018). Spatial and temporal evolution of natural and anthropogenic dust events over northern China. *Scientific Reports*, *8*(1), 2141, https://doi.org/10.1038/s41598-018-20382-5

Wang, X., Wen, H., Shi, J., Bi, J., Huang, Z., Zhang, B., Zhou, T., et al. (2018). Optical and microphysical properties of natural mineral dust and anthropogenic soil dust near dust source regions over northwestern China. *Atmospheric Chemistry and Physics*, *18*(3), 2119–2138, https://doi.org/10.5194/acp-18-2119-2018

Wang, Y., Ma, P.-L., Jiang, J., Su, H., & Rasch, P. (2016). Towards reconciling the influence of atmospheric aerosols and greenhouse gases on light precipitation changes in eastern China. *Journal of Geophysical Research: Atmospheres*, *121*, 5878–5887. https://doi.org/10.1002/2016JD024845

Wang, Y., Zhang, R. Y., & Saravanan, R. (2014). Asian pollution climatically modulates midlatitude cyclones following hierarchical modeling and observational analysis. *Nature Communications*, *5*(1). https://doi.org/10.1038/ncomms4098

Wang, Y. S., Li, Y., Wang, L. L., Liu, Z. R., Ji, D. S., Tang, G. Q., Zhang, J. K., et al. (2014). Mechanism for the formation of the January 2013 heavy haze pollution episode over central and eastern China. *Science China Earth Sciences*, *57*(1), 14–25. https://doi.org/10.1007/s11430-013-4773-4

Woody, M. C., Baker, K. R., Hayes, P. L., Jimenez, J. L., Koo, B., & Pye, H. O. T. (2016). Understanding sources of organic aerosol during CalNex-2010 using the CMAQ-VBS. *Atmospheric Chemistry and Physics*, *16*(6), 4081–4100. https://doi.org/10.5194/acp-16-4081-2016

Xu, P., Chen, Y., & Ye, X. (2013). Haze, air pollution, and health in China. *The Lancet*, *382*(9910), 2067. https://doi.org/10.1016/S0140-6736(13)62693-8)

Yang, X., Zhao, C., Guo, J., & Wang, Y. (2016). Intensification of aerosol pollution associated with its feedback with surface solar radiation and winds in Beijing. *Journal of Geophysical Research: Atmospheres*, *121*, 4093–4099. https://doi.org/10.1002/2015JD024645

Zhang, H., Chen, G., Hu, J., Chen, S. H., Wiedinmyer, C., Kleeman, M., & Ying, Q. (2014). Evaluation of a seven-year air quality simulation using the Weather Research and Forecasting (WRF)/Community Multiscale Air Quality (CMAQ) models in the eastern United States. *Science of the Total Environment*, *473-474*, 275–285. https://doi.org/10.1016/j.scitotenv.2013.11.121

Zhang, Q., Quan, J., Tie, X., Li, X., Liu, Q., Gao, Y., & Zhao, D. (2015). Effects of meteorology and secondary particle formation on visibility during heavy haze events in Beijing, China. *Science of the Total Environment*, *502*, 578–584.

Zhang, R., Khalizov, A. F., Wang, L., Hu, M., & Wen, X. (2012). Nucleation and growth of nanoparticles in the atmosphere. *Chemical Reviews*, *112*, 1957–2011.

Zhang, R., Wang, G., Guo, S., Zamora, M. L., Ying, Q., Lin, Y., et al. (2015). Formation of urban fine particulate matter. *Chemical Reviews*, *115*(10), 3803–3855. https://doi.org/10.1021/acs.chemrev.5b00067

Zhang, R. H., Li, Q., & Zhang, R. N. (2014). Meteorological conditions for the persistent severe fog and haze event over eastern China in January 2013. *Science China Earth Sciences*, *57*(1), 26–35. https://doi.org/10.1007/s11430-013-4774-3

Zhang, Y. X., Sheesley, R. J., Schauer, J. J., Lewandowski, M., Jaoui, M., Offenberg, J. H., et al. (2009). Source apportionment of primary and secondary organic aerosols using positive matrix factorization (PMF) of molecular markers. *Atmospheric Environment*, *43*(34), 5567–5574. https://doi.org/10.1016/j.atmosenv.2009.02.047

Zhao, C., Andrews, A. E., Bianco, L., Eluszkiewicz, J., Hirsch, A., MacDonald, C., et al. (2009). Atmospheric inverse estimates of methane emissions from central California. *Journal of Geophysical Research*, *114*, D16302. https://doi.org/10.1029/2008JD011671

Zhao, C., Lin, Y., Wu, F., Wang, Y., Li, Z., Rosenfeld, D., & Wang, Y. (2018). Enlarging rainfall area of tropical cyclones by atmospheric aerosols. *Geophysical Research Letters*, *45*, 8604–8611. https://doi.org/10.1029/2018GL079427

Zhao, X. J., Zhao, P. S., Xu, J., Meng, W., Pu, W. W., Dong, F., et al. (2013). Analysis of a winter regional haze event and its formation mechanism in the North China plain. *Atmospheric Chemistry and Physics*, *13*(11), 5685–5696. https://doi.org/10.5194/acp-13-5685-2013

Zheng, G. J., Duan, F. K., Su, H., Ma, Y. L., Cheng, Y., Zheng, B., et al. (2015). Exploring the severe winter haze in Beijing: The impact of synoptic weather, regional transport and heterogeneous reactions. *Atmospheric Chemistry and Physics*, *15*(6), 2969–2983. https://doi.org/10.5194/acp-15-2969-2015